Supplementary Material (ESI) for CrystEngComm 2019

Dual-responsive luminescent sensor based on water-stable Cd(II)-MOF for highly selective and sensitive detection of acetylacetone and $Cr_2O_7^{2-}$ in aqueous solution

Ying-Jie Yang, Yue-Hua Li, Dong Liu, Guang-Hua Cui*

College of Chemical Engineering, Hebei Key Laboratory for Environment Photocatalytic and Electrocatalytic Materials, North China University of Science and Technology, No. 21 Bohai Road, Caofeidian new-city, Tangshan, Hebei, 063210, P. R. China

*Corresponding author: Guang-Hua Cui

Fax: +86-315-8805462, Tel: +86-315-8805460.

E-mail: tscghua@126.com

Table S1 Crystal data and structure refinements for **1** and **2**.

Table S2(a) Selected Bond Lengths [Å] and Angles [º] for the **1**； **(b)** Selected Bond Lengths [Å] and Angles [º] for the **2**.

Table S3 The BET surface area and porosity of **1** and **2**.

Fig. S1 The two coordination modes of 1,4-NDC^{2-} ligands to form a $[Cd_2(1,4\text{-}NDC^{2-})_2]_n$ unit.

Fig. S2 (a) Each $[Cd_2(1,4\text{-}NDC^{2-})_2]_n$ unit binds to adjacent units to form a 3D framework; **(b)** The L1 ligands bridge two Cd(II) ions.

Fig. S3 Topological representation of the **lvt** network in **1** with $[Cd_2(1,4\text{-}NDC^{2-})_2]_n$ units selected as nodes.

Fig. S4 (a) The 1D waved chain $[Cd(1,4\text{-}NDC^{2-})]_n$ of **2**; **(b)** The similar "V" shape 1D chain $[Cd(L2)]_n$ of **2**.

Fig. S5 The simulated from single-crystal data, obtained from the experiment powder X-ray diffraction patterns of **1** and **2**.

Fig. S6 The TG curves of **1** and **2**.

Fig. S7 PXRD patterns of Cd(II)-MOFs (**a** = MOF-**1**; **b** = MOF-**2**) in different pH values in the range of 3-13.

Fig. S8 PXRD patterns of Cd(II)-MOFs (**a** = MOF-**1**; **b** = MOF-**2**) soaking in aqueous solution for 30 days.

Fig. S9 Comparison of the quenching efficiency relative of **1** in different small organic molecules (the luminescence intensity of **1** in aqueous solution is the original value).

Fig. S10 The luminescence intensity of **1** after sensing experiments (**a** = ACAC; **b** = $Cr_2O_7^{2-}$) five runs of recycling.

Fig. S11 The PXRD patterns (**a** = **1** after sensing ACAC for five cycles in H_2O; **b** = **1** after sensing $Cr_2O_7^{2-}$ ion for five cycles in H_2O).

Fig. S12 Comparison of the quenching efficiency relative of **1** in aqueous solution in the presence of different ions (**a** = metal ions; **b** = anions, the luminescence intensity of **1** in aqueous solution is the original value).

Fig. S13 Emission intensities of **1** dispersed in the aqueous solution of $Cr_2O_7^{2-}$ in the presence of different ions.

Fig. S14 IR spectra (**a** = powder of **1**; **b** = powder of **1** in H_2O; **c** = **1** after sensing ACAC for five cycles in H_2O; **d** = **1** after sensing $Cr_2O_7^{2-}$ ion for five cycles in H_2O).

Fig. S15 The EDX patterns (**a** = powder of **1**; **b** = **1** after sensing for ACAC for five cycles in H_2O; **c** = **1** after sensing $Cr_2O_7^{2-}$ ion for five cycles in H_2O).

Fig. S16 The UV-vis spectra **(a** = small organic molecules; **b** = metal ions; **c** = anions and the excitation spectra of **1**).

Table S1 Crystal data and structure refinements for **1** and **2**

MOF	**1**	**2**
Chemical formula	$C_{42}H_{28}N_4O_8Cd_2$	$C_{32}H_{26}N_4O_4Cd$
Formula weight	941.48	642.97
Crystal system	Monoclinic	Monoclinic
Space group	$P2_1/n$	$P2_1/c$
a (Å)	20.577(1)	15.503(9)
b (Å)	7.636(5)	10.572(6)
c (Å)	20.577(6)	18.453(1)
α (°)	90	90
β (°)	94.06(1)	107.03(1)
γ (°)	90	90
V (Å^3)	3225.0(4)	2891.7(3)
Z	4	4
D_{calcd} (g/cm^3)	1.939	1.477
Absorption coefficient, mm^{-1}	1.389	0.799
F(000)	1872	1304
Crystal size, mm	0.25 × 0.22 × 0.21	0.20 × 0.18 × 0.17
θ range, deg	2.281~28.320	2.246~28.326
Index range h, k, l	-27/27, -10/10, -27/27	-20/16, -14/14, -24/24
Reflections collected	57441	40688
Independent reflections (R_{int})	7972(0.0291)	7155 (0.0240)
Data/restraint/parameters	7972/ 6 / 516	7155 / 0 / 372
Goodness-of-fit on F^2	1.027	1.079
Final R_1, wR_2 ($I > 2\sigma(I)$)	0.0211, 0.0566	0.0267, 0.0996
Largest diff. peak and hole	1.523, -0.805	0.418, -0.987

Table S2(a) Selected Bond Lengths [Å] and Angles [º] for the **1**

Parameter	Value	Parameter	Value
1			
Cd(1)–O(1)	2.270(2)	Cd(1)–O(7)A	2.258(2)
Cd(1)–O(8)A	2.576(2)	Cd(1)–O(8)B	2.323(2)
Cd(1)–O(2)C	2.338(2)	Cd(1)–N(1)	2.241(2)
Cd(2)–O(4)	2.210(2)	Cd(2)–O(5)	2.279(2)
Cd(2)–O(3)D	2.319(2)	Cd(2)–O(6)D	2.366(2)
Cd(2)–N(2)	2.224(2)		
N(1)–Cd(1)–O(7)A	166.5(8)	N(1)–Cd(1)–O(1)	97.5(7)
O(7)A–Cd(1)–O(1)	85.6(8)	N(1)–Cd(1)–O(8)B	100.7(7)
O(7)A–Cd(1)–O(8)B	92.5(6)	O(1)–Cd(1)–O(8)B	87.8(7)
N(1)–Cd(1)–O(2)C	85.4(7)	O(7)A–Cd(1)–O(2)C	93.5(8)
O(1)–Cd(1)–O(2)C	171.2(8)	O(8)B–Cd(1)–O(2)C	83.4(7)
N(1)–Cd(1)–O(8)A	113.1(7)	O(7)A–Cd(1)–O(8)A	53.8(6)
O(1)–Cd(1)–O(8)A	87.6(6)	O(8)B–Cd(1)–O(8)A	146.2(4)
O(2)C–Cd(1)–O(8)A	99.0(6)	O(4)–Cd(2)–N(2)	160.4(8)
O(4)–Cd(2)–O(5)	92.9(8)	N(2)–Cd(2)–O(5)	102.6(7)
O(4)–Cd(2)–O(3)D	90.1 (6)	N(2)–Cd(2)–O(3)D	101.2(7)
O(5)–Cd(2)–O(3)D	92.2(7)	O(4)–Cd(2)–O(6)D	85.9(7)
N(2)–Cd(2)–O(6)D	80.5(7)	O(5)–Cd(2)–O(6)D	171.7(7)
O(3)D–Cd(2)–O(6)D	79.6(7)		

Symmetry codes for **1**: A = *x*+1/2, -*y*+3/2, *z*-1/2; B = -*x*+1, -*y*+1, -*z*+1; C = -*x*+3/2, *y*-1/2, -*z*+1/2; D = -*x*+1/2, *y*-1/2, -*z*+1/2.

Table S2(b) Selected Bond Lengths [Å] and Angles [º] for the **2**

Parameter	Value	Parameter	Value
2			
Cd(1)–O(1)	2.243(2)	Cd(1)–O(2)	2.463(2)
Cd(1)–O(3)A	2.234(2)	Cd(1)–O(4)A	2.526(2)
Cd(1)–N(1)	2.292(2)	Cd(1)–N(3)	2.325(2)
O(3)A–Cd(1)–O(1)	141.6(8)	O(3)A–Cd(1)–N(1)	98.6(7)
O(1)–Cd(1)–N(1)	114.6(7)	O(3)A–Cd(1)–N(3)	104.9(8)
O(1)–Cd(1)–N(3)	95.5(6)	N(1)–Cd(1)–N(3)	87.8(6)
O(3)A–Cd(1)–O(2)	107.8(9)	O(1)–Cd(1)–O(2)	54.4(7)
N(1)–Cd(1)–O(2)	92.7(7)	N(3)–Cd(1)–O(2)	146.8(7)
O(3)A–Cd(1)–O(4)A	53.8(6)	O(1)–Cd(1)–O(4)A	89.3(7)
N(1)–Cd(1)–O(4)A	150.7(6)	N(3)–Cd(1)–O(4)A	107.5(7)
O(2)–Cd(1)–O(4)A	87.8(8)		

Symmetry codes for **2**: A = *x*, -*y*+3/2, *z*-1/2.

Table S3 The BET surface area and porosity of **1** and **2**

MOFs	BET surface area (m^2/g)	Porosity (cm^3/g)
1	3.414	0.0003
2	0.453	0.0009

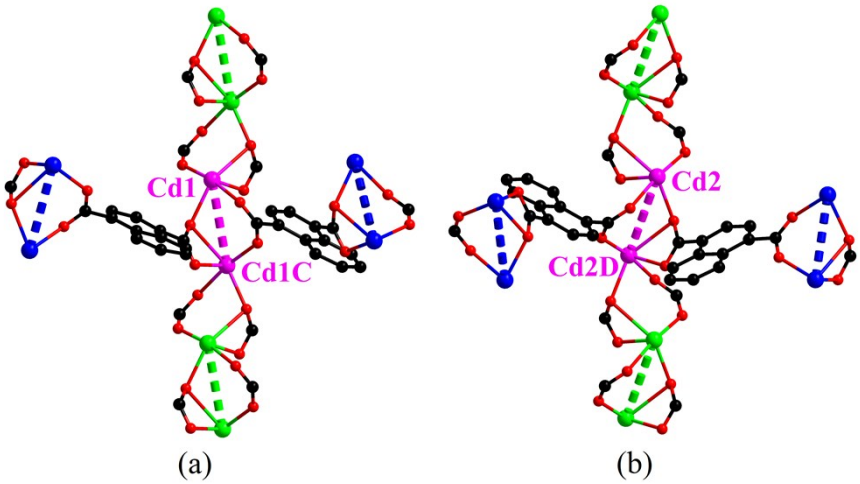

Fig. S1 The two coordination modes of 1,4-NDC^{2-} ligands to form a $[Cd_2(1,4\text{-}NDC^{2-})_2]_n$ unit.

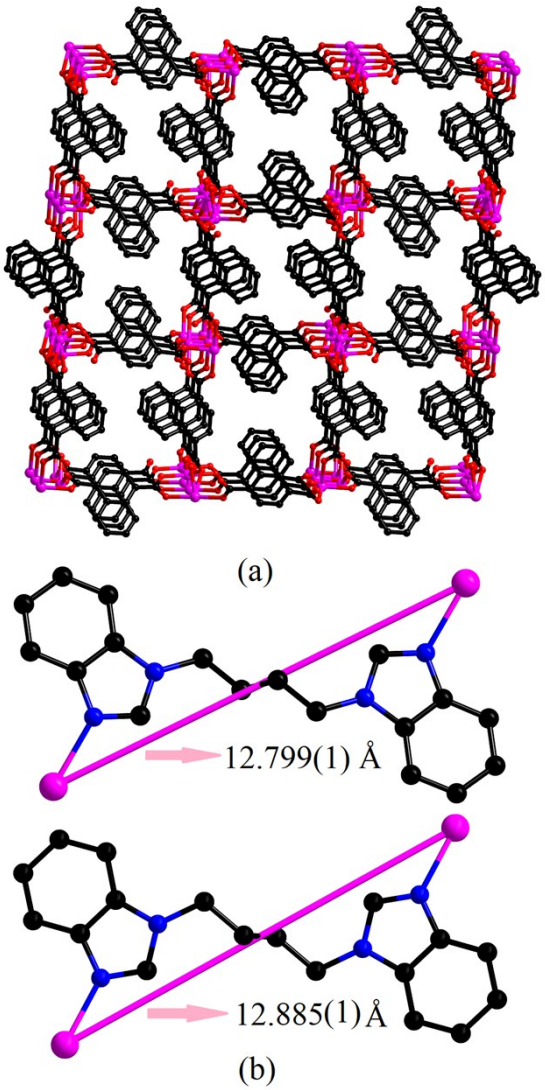

Fig. S2 (a) Each $[Cd_2(1,4\text{-}NDC^{2-})_2]_n$ unit binds to adjacent units to form a 3D framework; **(b)** The L1 ligands bridge two Cd(II) ions.

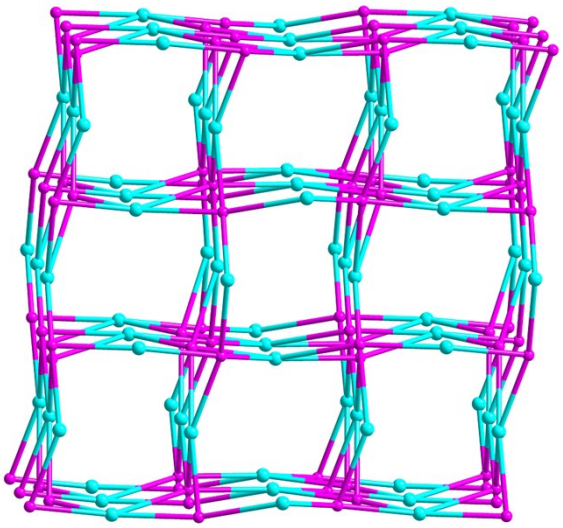

Fig. S3 Topological representation of the **lvt** network in **1** with $[Cd_2(1,4\text{-}NDC^{2-})_2]_n$ units selected as nodes.

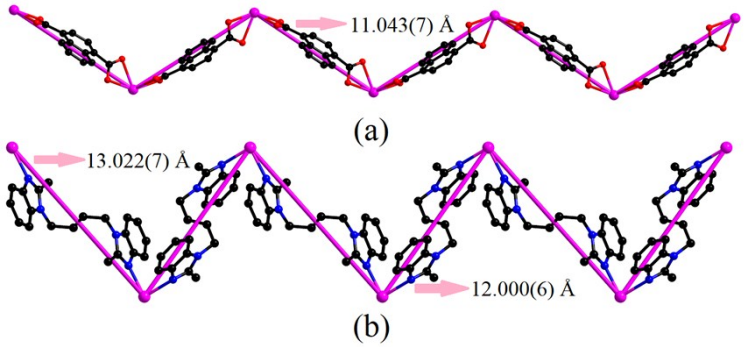

Fig. S4 (a) The 1D waved chain $[Cd(1,4\text{-NDC})]_n$ of **2**; **(b)** The similar "V" shape 1D chain $[Cd(L2)]_n$ of **2**.

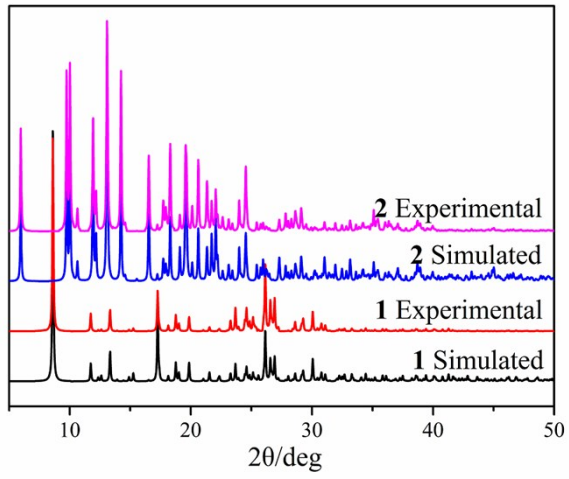

Fig. S5 The simulated from single-crystal data, obtained from the experiment powder X-ray diffraction patterns of **1** and **2**.

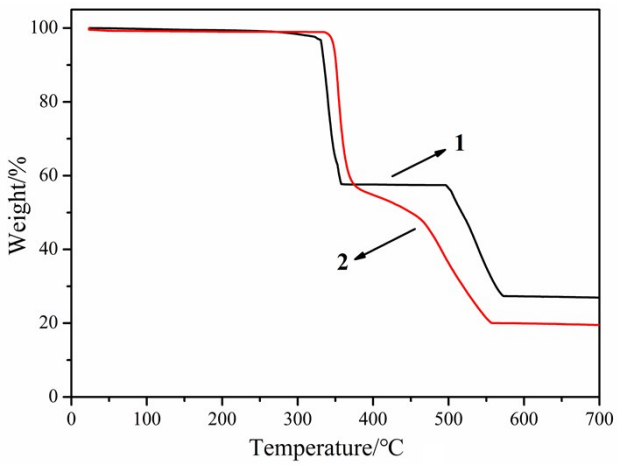

Fig. S6 The TG curves of **1** and **2**.

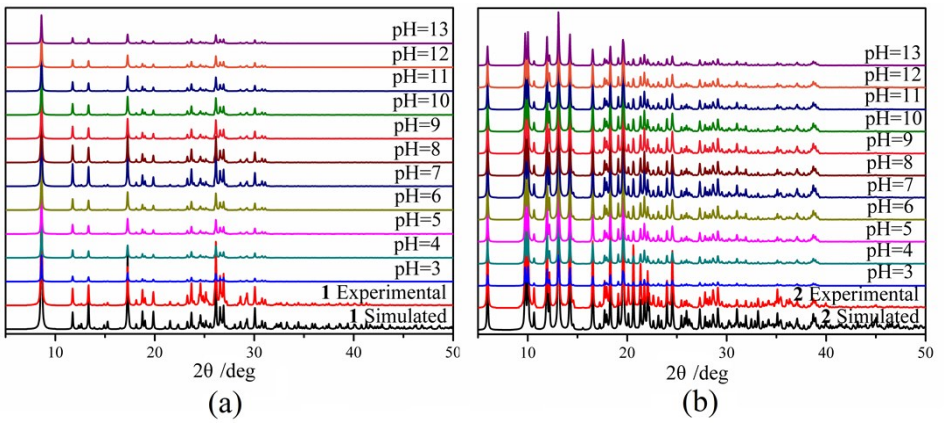

Fig. S7 PXRD patterns of Cd(II)-MOFs (**a** = MOF-**1**; **b** = MOF-**2**) in different pH values in the range of 3~13.

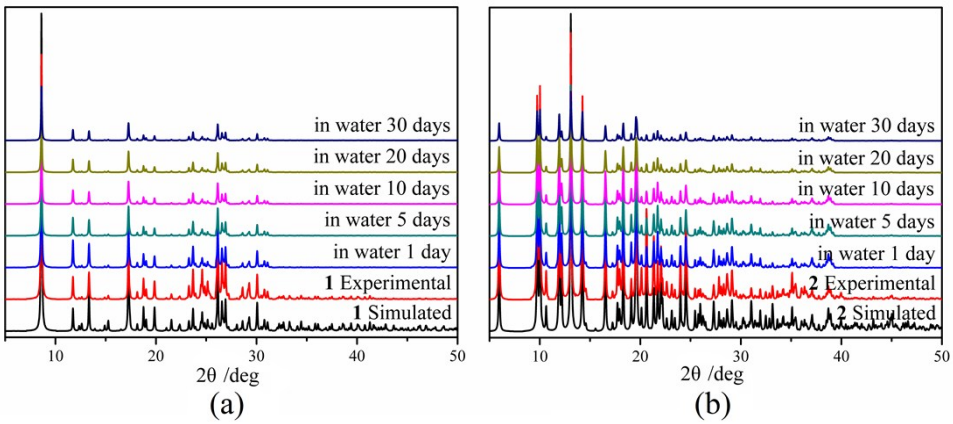

Fig. S8 PXRD patterns of Cd(II)-MOFs (**a** = MOF-**1**; **b** = MOF-**2**) soaking in aqueous solution for 30 days.

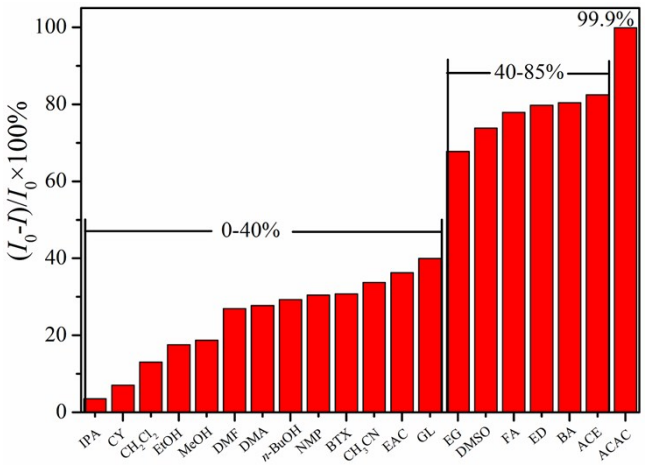

Fig. S9 Comparison of the quenching efficiency relative of **1** in different small organic molecules (the luminescence intensity of **1** in aqueous solution is the original value).

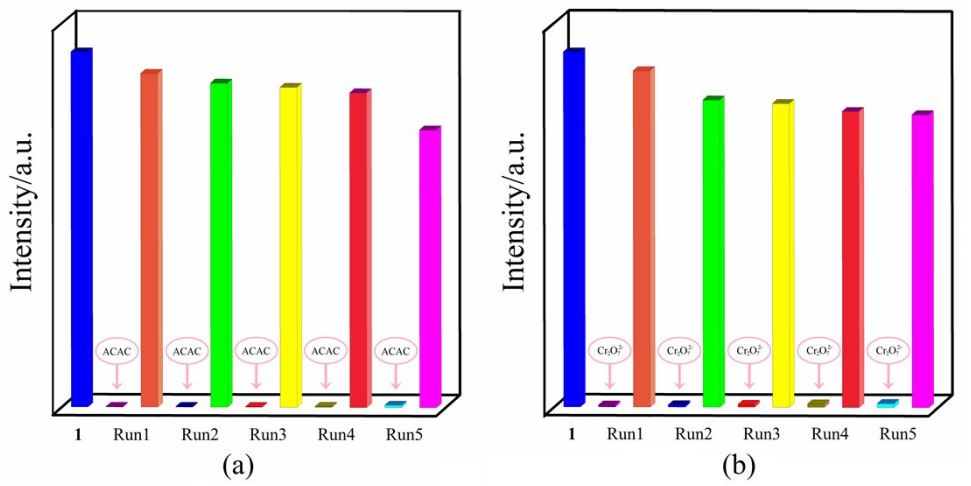

Fig. S10 The luminescence intensity of **1** after sensing experiments (**a** = ACAC; **b** = $Cr_2O_7^{2-}$) five runs of recycling.

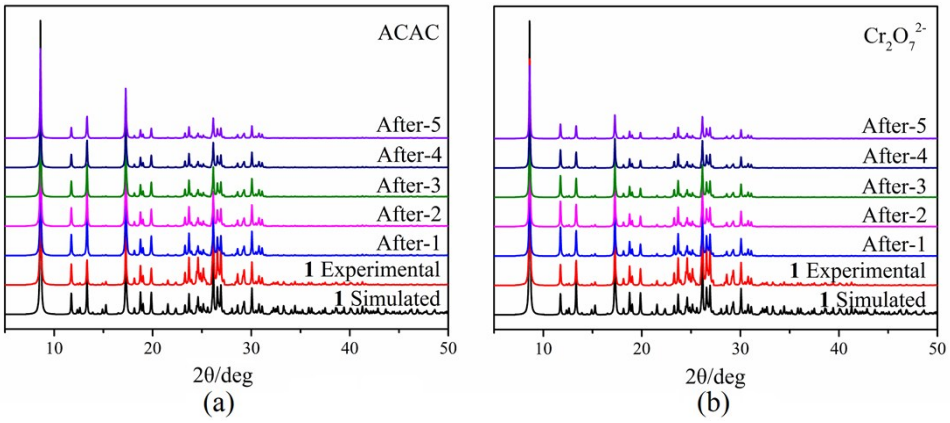

Fig. S11 The PXRD patterns (**a** = **1** after sensing ACAC for five cycles in H_2O; **b** = **1** after sensing $Cr_2O_7^{2-}$ ion for five cycles in H_2O).

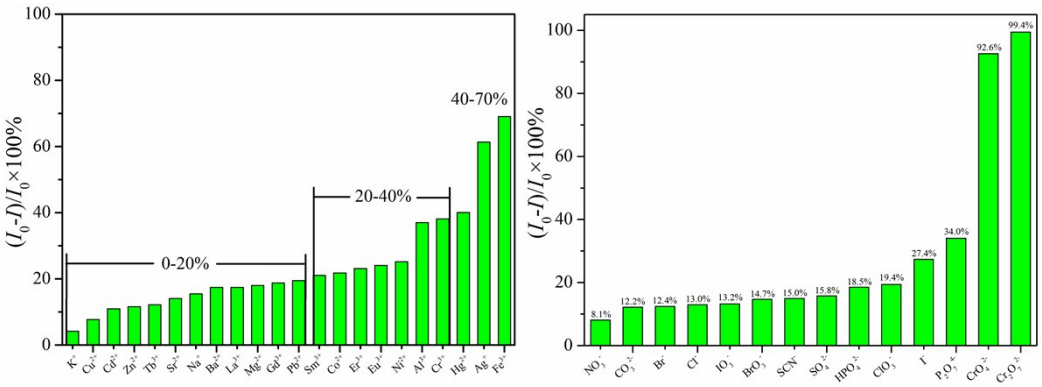

Fig. S12 Comparison of the quenching efficiency relative of **1** in aqueous solution in the presence of different ions (**a** = metal ions; **b** = anions, the luminescence intensity of **1** in aqueous solution is the original value).

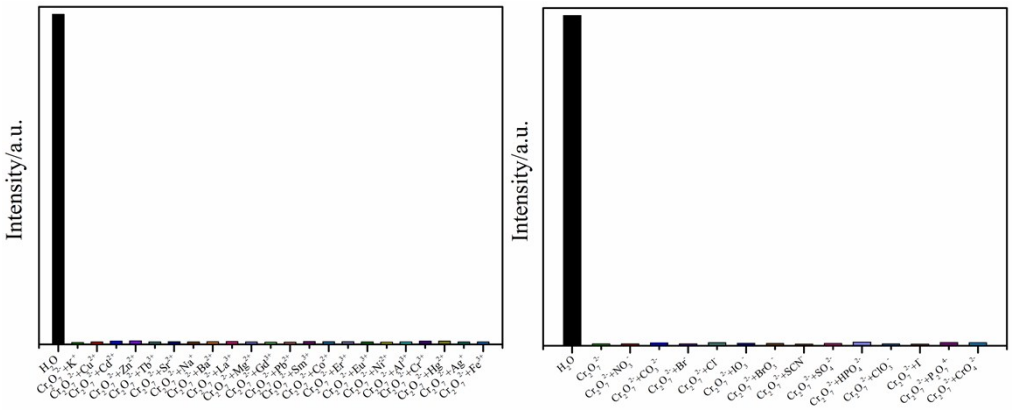

Fig. S13 Emission intensities of **1** dispersed in the aqueous solution of $Cr_2O_7^{2-}$ in the presence of different ions.

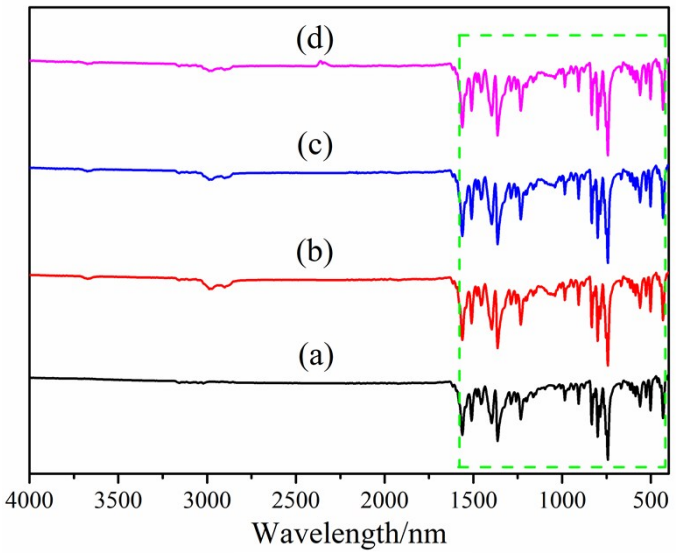

Fig. S14 IR spectra (**a** = powder of **1**; **b** = powder of **1** in H_2O; **c** = **1** after sensing ACAC for five cycles in H_2O; **d** = **1** after sensing $Cr_2O_7^{2-}$ ion for five cycles in H_2O).

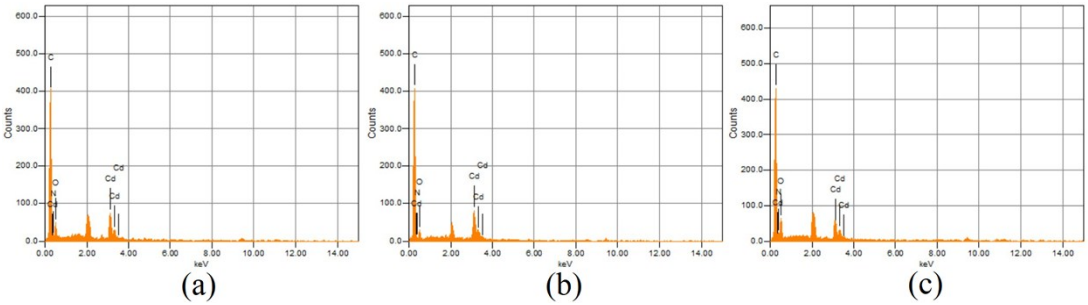

Fig. S15 The EDX patterns (**a** = powder of **1**; **b** = **1** after sensing for ACAC for five cycles in H_2O; **c** = **1** after sensing $Cr_2O_7^{2-}$ ion for five cycles in H_2O).

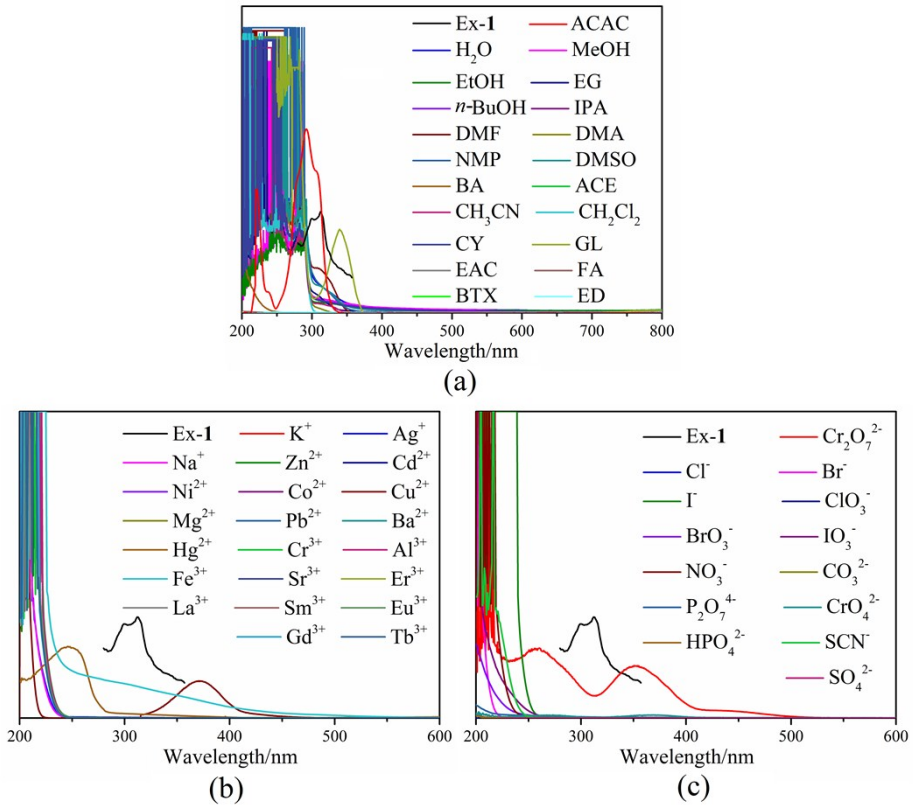

Fig. S16 The UV-vis spectra (**a** = small organic molecules; **b** = metal ions; **c** = anions and the excitation spectra of **1**).